Plasma Ion Evolution in the Wake of a High-Intensity Ultrashort Laser Pulse

M. Borghesi,[1] S. V. Bulanov,[1,2,*] T. Zh. Esirkepov,[2,†] S. Fritzler,[3] S. Kar,[1] T. V. Liseikina,[4] V. Malka,[3] F. Pegoraro,[4] L. Romagnani,[1] J. P. Rousseau,[3] A. Schiavi,[5] O. Willi,[6] and A. V. Zayats[1]

[1]*School of Mathematics and Physics, The Queen's University of Belfast, Belfast BT7 1NN, United Kingdom*
[2]*Moscow Institute of Physics and Technology, Dolgoprudnyi 141700, Russia*
[3]*Laboratoire d' Optique Appliquee, ENSTA, 91128 Palaiseau, France*
[4]*University of Pisa and INFM, pz. Pontecorvo 2, Pisa 56100, Italy*
[5]*Department of Energetics, University of Rome "La Sapienza", Rome, Italy*
[6]*Heinrich Heine Universität, Dusseldorf, Germany*
(Received 9 January 2004; published 17 May 2005)

Experimental investigations of the late-time ion structures formed in the wake of an ultrashort, intense laser pulse propagating in a tenuous plasma have been performed using the proton imaging technique. The pattern found in the wake of the laser pulse shows unexpectedly regular modulations inside a long, finite width channel. On the basis of extensive particle in cell simulations of the plasma evolution in the wake of the pulse, we interpret this pattern as due to ion modulations developed during a two-stream instability excited by the return electric current generated by the wakefield.

DOI: 10.1103/PhysRevLett.94.195003 PACS numbers: 52.38.−r, 52.27.Ny, 52.35.Sb, 52.65.Rr

The dynamics of Langmuir waves in plasmas, their turbulence and decay and the subsequent plasma evolution [1] are topics of high interest for a wide class of plasma phenomena, including astrophysical plasmas [2], beam-plasma interactions [3] and laser-plasma interactions relevant to Inertial Confinement Fusion [4]. In the context of ultrashort, high-intensity laser-plasma interaction physics, Langmuir waves excited by ultrashort, high-intensity laser pulses are at the basis of innovative and highly promising electron-acceleration schemes [5].

As is well known, a laser pulse with a length of the order of, or shorter than, a plasma oscillation wavelength $\lambda_p = 2\pi c/\omega_{pe}$ efficiently generates a Langmuir wave in its wake. In a cold plasma a Langmuir wave has zero group velocity so that, once generated, it might be expected to remain in the plasma. However nonlinear processes eventually change the $\mathbf{k}_p$ spectrum of the wake wave, as shown by the equation $\partial_t \mathbf{k}_p = -\nabla\omega_{pe}$, which gives the time evolution of the wave number at a fixed position in inhomogeneous media (see Ref. [6]). In the presence of a plasma inhomogeneity, either induced by the laser itself or preestablished, this leads to eventual wave breaking even for small amplitudes of the wake wave and low plasma densities because the wake wavelength $\lambda_p = 2\pi/|k_p|$ will eventually decrease down to a value equal to the quiver displacement of the electrons [7].

For short laser pulses of moderate intensity, i.e., for dimensionless pulse amplitudes much smaller than the square root of the mass ratio, $eE/(m_e\omega c) \ll (m_p/m_e)^{1/2}$, the generation of the wakefield can be described using the approximation of fixed ions [8]. However on a time scale longer than the pulse duration, even in the case of moderate pulse intensities, the ponderomotive pressure of the wakefield left behind the laser pulse will displace the ions perpendicularly to the laser beam axis and form a plasma channel [9]. The evolution of the plasma channel occurs on the ion time scale, which is much longer than the pulse length and the wakefield period (up to tens of picoseconds depending on the plasma density).

This Letter presents results of experimental investigations of late-time ion structures formed in the wake of an ultrashort, intense laser pulse propagating in a tenuous plasma. A surprisingly regular ion density modulation extending for several hundreds of microns in the wake of the pulse has been observed for the first time, via the associated electrostatic field, using the proton imaging technique [10]. The physical process responsible for the formation of this pattern has been investigated with extensive particle in cell (PIC) simulations of the plasma evolution over long time scales. On the basis of the PIC results and of theoretical considerations, we interpret this pattern as due to ion modulations caused by a two-stream instability induced by the return electric current generated by the wakefield. These results demonstrate the existence of an intermediate stage of the plasma dynamics following the electrostatic wake decay where regular, quasiperiodic, long-lived ion structures are formed.

The experiment was carried out at the LOA Laboratory, employing the Ti:Sa Salle Jaune laser [11] operating in the chirped pulse amplification mode (CPA) and delivering up to 2 J in 35 fs laser pulses at $\lambda = 0.8\ \mu$m. The laser pulse was split in two separate pulses after amplification and recompressed under vacuum with two separate sets of gratings. This allowed the use of two pulses (CPA_1 and CPA_2) of 35 fs duration. As in previous experiments [10], the CPA_1 pulse was used to accelerate a beam of MeV protons from a thin (6–10 μm) Al foil. The proton beam pulse was used as a transverse particle probe to diagnose the interaction of the CPA_2 pulse with a secondary target, or a preformed plasma. This diagnostic scheme for the detection of electromagnetic (EM) fields has been already

employed in some experiments to study the response of plasmas and solid targets to ultraintense, ps irradiation [12]. For a schematic of the experimental arrangement see Fig. 1 of Ref. [10]. The distance between the proton foil and the interaction axis was $d = 1.5$ mm, while the detector was placed at $L = 21$ mm from the proton foil, yielding a point projection magnification $M \approx 14$. CPA_1 had energy up to 1.2 J, and was focused to intensities of about $I = 5 \times 10^{19}$ W/cm^2 onto a 6 μm Al foil. CPA_2 had 0.5 J energy, and was focused with an $f/3$ off-axis parabola (I at focus $\approx 5 \times 10^{19}$ W/cm^2) on a second target. The delay between the two CPA pulses could be controlled with ps precision. The LOA high-intensity pulse is preceded by an amplified spontaneous emission (ASE) pedestal starting about 4 ns before the pulse peak, with a main-to-prepulse contrast ratio better than 10^7. Because of the effect of the ASE forming a cold plasma atmosphere ahead of the high-intensity laser pulse, the main pulse interacts with a preformed plasma rather than with a solid target [13]. The experiment was performed in a vacuum chamber evacuated down to a pressure in the range $0.1–1 \times 10^{-3}$ bar. Under these conditions, the laser pulses propagate through a tenuous air gas on their way to the intended targets. The proton beam produced using the CPA_1 pulse contained energies up to about 5 MeV. The detector employed to reveal the proton beam intensity cross section and the modulations imprinted after propagation through the plasma was the CR-39 nuclear track detector [14]. The detector was shielded with a 75 μm Al foil, in order to select protons with energy around 3 MeV. The tracks produced on the CR39 by the single protons can be revealed by etching it in a NaOH solution under controlled conditions after exposure. As a result, one can map on the detector surface the track density, yielding the proton density distribution across the beam cross section. The CPA_2 beam was focused onto the surface of Al or CH foils of variable thickness. The interaction region was probed with the proton beam at different times before and after the arrival of CPA_2 on target, with the aim of identifying the signature of plasma structures induced by the high-intensity propagation. Distortions in the proton density profile can be ascribed to EM field structures present in the plasma traversed by the interaction pulse. The spatial resolution (typically a few μm) with which the small scale EM structures can be mapped is related to the source emittance [15], while the temporal resolution (typically a few ps) is given by the transit time of the protons across the region where the fields are present. Several structures were observed in the data. In this letter we concentrate our attention on a striking feature observed for tens of ps after the pulse propagation in the tenuous plasma preceding the target in the wake of the focusing pulse. In Fig. 1(a) a proton projection image of the region in front of the target taken 20 ps after the interaction is shown. Frame (a) is a reflection scan of the etched CR39 (darker regions correspond to higher proton densities). The spatial scale used in Fig. 1(a) refers to the dimensions in the interaction plane. A clear modulated pattern is observed within the cone of the focusing laser pulse along the propagation direction. The pattern extends for several hundred of microns and terminates at a distance of about 300 μm from the intended focus, when it encounters a circular structure surrounding the focal position on the target. The period of the pattern varies slowly along the propagation axis and is of the order of $\approx 25–30$ μm. The modulation in proton density corresponding to two peaks of the quasiperiodic struc-

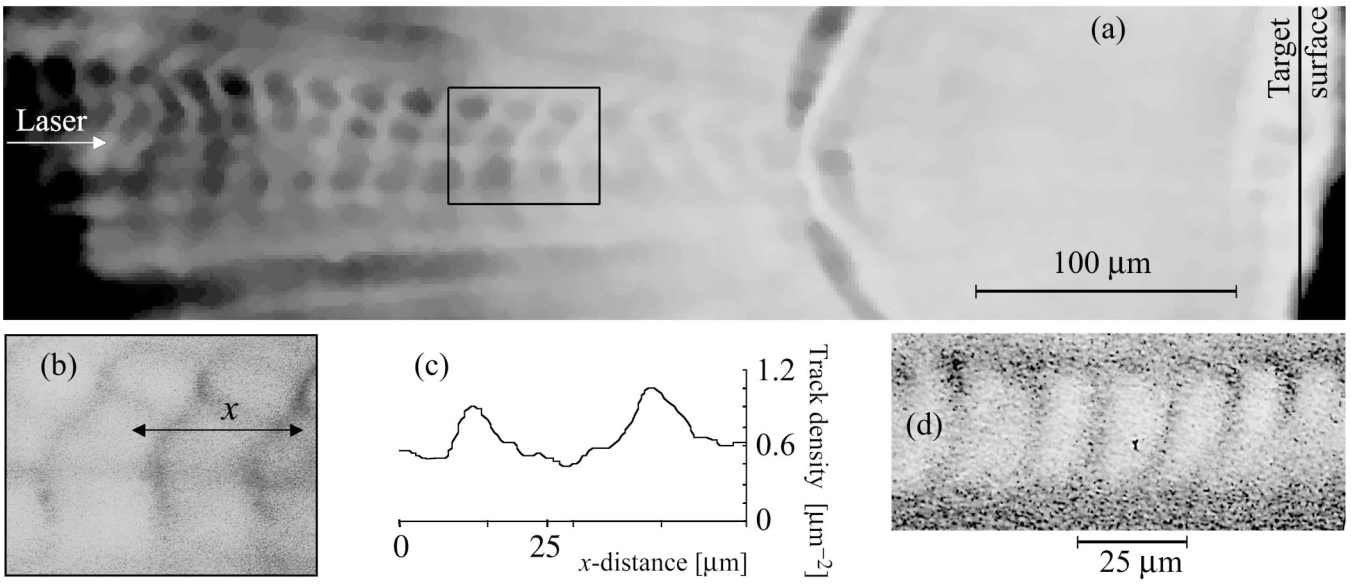

FIG. 1. (a) Proton projection image of the region in front of the laser-irradiated target, taken 20 ps after the interaction. The picture is a reflection scan of the exposed CR 39; (b) Detail of the image in frame (a), (c) Profile of the proton track density along the direction indicated by the arrow in (a); (d) Detail of the pattern observed at the back of a 0.9 μm Mylar target 20 ps after the interaction. The detail shown was located at a distance of about 200 μm from the original target plane.

ture is shown in Fig. 1(c). The profile has been obtained by atomic force microscopy analysis of the CR39 sample [16]. In order to estimate the plasma density at which the structure is seen some considerations are necessary. Hydrodynamic simulations, carried out with the 2D hydrocode POLLUX [17] using the experimental parameters for the prepulse, provide an indication of the radial extent of the preplasma formed by the ASE. The plasma with density higher than 10^{17} cm^{-3} is contained within a region with radius smaller than 300 μm. This suggests that the density in the region where the periodic structure is observed is lower than this value. On the other hand, the tenuous air gas present inside the interaction chamber will be ionized via tunnel ionization by the rising edge of the pulse. If one considers tunnel ionization of N_2 (the main constituent of air), consistent with the intensity of the focusing pulse in the region under consideration (10^{17}–10^{18} W/cm^2) [18], one can estimate a ionization state of 5 and an electron density in the range of 10^{16}–10^{17} cm^{-3}. The curved structure observed at the right edge of Fig. 1(a) is likely to be a signature (e.g., a propagating shock wave) of the interface between the plasma ablated from the target and the tenuous gas or plasma surrounding the target. The modular pattern is a repeatable feature of the plasma evolution and has been observed from a few ps up to 70–80 ps after the interaction. In shots performed using thin foils (e.g., 1 μm thick mylar), similar modular patterns are observed at the back of the target [see Fig. 1(d)]. One should note that in the case of thin foils, the ASE explodes the foil [13] and the laser propagates through the resulting underdense plasma.

Since in the region under observation the density is too low for significant scattering effects to take place, the periodic pattern must be imprinted onto the proton beam via an EM field structure. Assuming that the proton deflection $\xi_\perp$ arises from an electric field $\mathbf{E}_p$, slowly varying on the proton crossing time, $\xi_\perp$ can be estimated as $\xi_\perp \approx eL(\int_0^l \mathbf{E}_{p,\perp} dz/m_p v_p^2)$. The modulations in the proton density image arise from the differential deflection of the proton trajectories and are thus given by $\delta n/n_0 \approx -(\mathrm{div}_\perp \xi_\perp)(L/l)$ where L is the distance between the detector and the plasma, l is the transverse size of the wake, v_p is the proton velocity, $\mathrm{div}_\perp \xi_\perp = \partial_x \xi_x + \partial_y \xi_y$, and we have assumed $|\mathrm{div}_\perp \xi_\perp| \ll 1$. We see that in this limit the probe proton density modulation measures the charge density ρ averaged along the proton beam path: $\delta n/n_0 \approx 4\pi e\rho l L/m_p v_p^2$. From the measured values of the proton density modulations we obtain $E_{p,\perp} \approx 3 \times 10^8$ V/m.

In order to investigate the physical mechanisms which could be responsible for the formation of such patterns, extensive two-dimensional PIC simulations of the long time evolution of the plasma in the wake of a short, high-intensity, laser pulse propagating in an underdense plasma have been performed with the use of the REMP code [19]. In the simulations presented here a linearly s-polarized laser pulse with dimensionless amplitude $a = eE_l/(m_e \omega c) = 1$, corresponding to the peak intensity $I = 2.14 \times 10^{18}$ W/cm^2 for a $\lambda = 0.8$ μm laser, propagates along the x axis. The laser pulse has a Gaussian envelope with FWHM size $15\lambda \times 70\lambda$, which meets the requirements of the resonant wakefield generation. The plasma density is $n_0 = 10^{-3} n_{cr}$, which corresponds to $\omega_{pe}/\omega = \lambda/\lambda_p = 0.0316$. Because of limitations in computational power it is difficult to perform simulations with a substantially lower plasma density. Ions and electrons have the same absolute charge and mass ratio $m_i/m_e = 1836$. The simulation box has 3500×1750 grid points with 0.1λ mesh size. The total number of quasiparticles is above 6×10^6. The boundary conditions are absorbing in all directions for both the EM radiation and the quasiparticles. The space and time unit are the wavelength λ and the period $2\pi/\omega$ of the incident radiation. In Fig. 2 we show the ion density distribution in the subdomain ($120 < x < 220$, $-30 < y < 30$) in the wake of the s-polarized pulse (with its electric field along the z axis) at $t = 2000$, long after the pulse has left the computation region. The ion density modulations along the line $y = 0$ are shown in Fig. 2(b). We see quasiperiodic structures in the pulse wake. Their longitudinal space scale λ_S is of the order of 10λ, approximately 10 times larger than the laser pulse wavelength but 3 times smaller than the wakefield wavelength λ_p. Similar patterns were observed in the simulations for a wide range of parameters. The ion pattern in Fig. 2 results from a sequence of plasma developments in the wake of the pulse. Our simulations show that in the initial stage, $10 < t < 300$, the laser pulse excites a Langmuir wake wave. At time $t \approx 300$ the Langmuir wake starts to decay due to wave-breaking. At $t \approx 450$ longitudinal ion density modulations start to form in the region near the left hand side of the

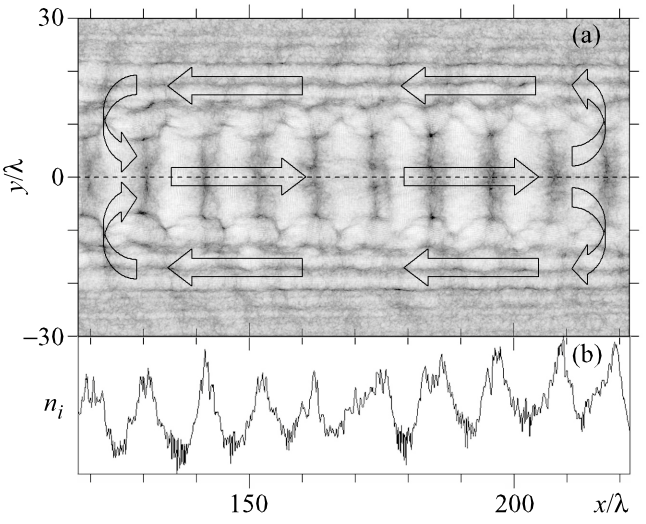

FIG. 2. (a) Ion density distribution in the (x, y) plane as obtained from the numerical simulations at $t = 2000$. A sketch of the large scale electron motion needed for the development of the Buneman instability is superimposed; (b) Ion density modulations at $y = 0$ along the pulse axis.

plasma slab where the decay of the Langmuir wave starts earlier. At first, they are shapeless and have a typical space scale between 1 and 1.5λ. Around $t \approx 500$ these short wavelength ion perturbations start to merge into a quasiperiodic pattern. Later, at $t \approx 750$, a distinct quasiperiodic pattern is formed seen in Fig. 2(a), which persists till $t \approx 2500$ when it starts to dissolve due to ion trajectory intersection and multistream motion. For a 0.8 μm laser this time corresponds to ≈ 6 ps.

The properties of these quasiperiodic ion wake structures may be interpreted in terms of the two-stream instability [20]. In this framework the ion density modulations arise from the development of the Buneman or ion-acoustic instability of the electrons in the return current. In the limit of cold counterstreaming electrons and ions we obtain for the dispersion equation of the Buneman instability $\varepsilon(\omega, k) = 1 - \omega_{pe}^2/[\gamma_e^3(\omega - k v_{\rm rc})^2] - \omega_{\rm pi}^2/\omega^2 = 0$, where $v_{\rm rc} < c$ is the return current streaming electron velocity, $\omega_{\rm pi} = (4\pi n_0 e^2/m_i)^{1/2}$ is the ion plasma frequency and $\gamma_e = (1 - v_{rc}^2/c^2)^{-1/2}$. The maximum growth rate $\omega'' = \omega_{pe}(3/\gamma_e)^{1/2}(m_e/16m_i)^{1/3}$ occurs for the ''resonant'' wave number $k_m = \omega_{pe}/v_{\rm rc}$, while the corresponding frequency is $\omega' = \omega_{pe}\gamma_e^{-1/2}\,(m_e/16m_i)^{1/3}$. For $v_{\rm rc} < c$ the wavelength $2\pi/k_m$ is substantially shorter than λ_p. Resonant unstable perturbations with $k \sim k_m$ grow until they saturate due to electron trapping that leads to electron heating. The instability can then evolve either as an ion-acoustic or a nonresonant Buneman mode. The nonresonant Buneman modes have almost zero frequency in the ion rest reference frame, in agreement with the results of the numerical simulations where the ion density modulations are observed not to propagate, and their linear growth rate is $\omega'' = k v_{\rm rc}(m_e/\gamma_e^3 m_i)^{1/2}$, from where we find $v_{\rm rc} \approx 0.2c$. In the nonlinear regime these modes lead to strong ion density modulations and eventually to ion trajectory self-intersection [21] in agreement with the process seen in the computer simulations.

From the simulation results we find the ion energy in the density patterns arising from the Buneman instability to be of the order of $\mathcal{E}_i \approx 10$ keV and the electric field in the plasma to be of the order of $E_p \approx 3 \times 10^9$ V/m. This is consistent with the expression $\mathcal{E}_i \approx 2eE_p/k$, which corresponds to the characteristic energy of an ion trapped in the electrostatic potential of the pattern. We notice that the development time of the pattern scales with the plasma density as $\sim n_0^{-1/2}$, which can explain why under the conditions of the experiment, where the plasma density is substantially lower, the ion wake pattern survives much longer. Taking into account that the electric field scales as $\sim n_0^{1/2}$, we also find agreement with the electric field value seen in the experiment. We notice that our computer simulations have provided no indication of the onset of a modulational instability [22].

The onset of the two-stream instability in the interaction between the plasma and the return current has been investigated also in Ref. [23] in connection with the problem of plasma heating by relativistic electron beams. The heating mechanism, which includes wave mixing and nonlinear wave breaking, was shown to result in the energy being transferred to the plasma ions. The experimental and simulation results discussed in our paper indicate that an intermediate regime can occur where regular, quasiperiodic long-lived ion structures are formed.

This work is supported by INTAS Grant No. 001-0233, by the EU Access Contract No. HPRI-1999-CT-00086, by EPSRC grant no. GR/R 65947, and by the QUB/IRCEP scheme.

*Also at APRC, JAERI, Kizu, Kyoto 619-0215, Japan, and General Physics Inst., RAS, Moscow 119991, Russia
†Also at APRC, JAERI, Kizu, Kyoto 619-0215, Japan

[1] M. V. Goldman, Rev. Mod. Phys. **56**, 709 (1984), and references therein.
[2] G. Thejappa *et al.*, J. Geophys. Res. **108**, 1139 (2003).
[3] B. Li *et al.*, Phys. Plasmas **10**, 2748 (2003).
[4] S. Depierreux *et al.*, Phys. Rev. Lett. **89**, 045001 (2002); C. G. R. Geddes *et al.*, Phys. Plasmas **10**, 3422 (2003).
[5] T. Tajima and J. M. Dawson, Phys. Rev. Lett. **43**, 267 (1979); S. P. D. Mangles *et al.*, Nature (London) **431**, 535 (2004); C. G. R. Geddes *et al.*, Nature (London) **431**, 538 (2004); J. Faure *et al.*, Nature (London) **431**, 541 (2004).
[6] G. B. Whitham, *Linear and Nonlinear Waves* (Wiley, New York, 1974).
[7] S. V. Bulanov *et al.*, Phys. Rev. Lett. **78**, 4205 (1997);S. V. Bulanov *et al.*, Phys. Rev. E **58**, R5257 (1998).
[8] A. G. Khachatryan, Phys. Rev. E **58**, 7799 (1998); S. V. Bulanov *et al.*, Plasma Phys. Rep. **25**, 701 (1999); L. M. Gorbunov *et al.*, Phys. Rev. E **65**, 036401 (2002).
[9] L. M. Gorbunov *et al.*, Phys. Rev. Lett. **86**, 3332 (2001).
[10] M. Borghesi *et al.*, Phys. Plasmas **9**, 2214 (2002); M. Borghesi *et al.*, Rev. Sci. Instrum. **74**, 1688 (2003).
[11] M. Pittman *et al.*, Appl. Phys. B **74**, 529 (2002).
[12] M. Borghesi *et al.*, Phys. Rev. Lett. **88**, 135002 (2002);M. Borghesi *et al.*, Appl. Phys. Lett. **82**, 1529 (2003).
[13] D. Giulietti *et al.*, Phys. Plasmas **9**, 3655 (2002); K. Matsukado *et al.*, Phys. Rev. Lett. **91**, 215001 (2003).
[14] F. H. Seguin *et al.*, Rev. Sci. Instrum. **74**, 975 (2003).
[15] M. Borghesi *et al.*, Phys. Rev. Lett. **92**, 055003 (2004); T. Cowan *et al.*, Phys. Rev. Lett. **92**, 204801 (2004).
[16] K. Amemiya *et al.*, Nucl. Instrum. Methods Phys. Res., Sect. B **159**, 75 (1999).
[17] G. J. Pert, J. Comput. Phys. **43**, 111 (1981).
[18] M. V. Ammosov *et al.*, Sov. Phys. JETP **64**, 1191 (1986).
[19] T. Zh. Esirkepov, Comput. Phys. Commun. **135**, 144 (2001).
[20] A. B. Mikhailovskii, *Theory of Plasma Instabilities* (Consultants Bureau, N.Y., 1974), Vol. 1.
[21] A. A. Galeev *et al.*, Zh. Eksp. Teor. Fiz. **81**, 572 (1981); S. V. Bulanov *et al.*, Sov. J. Plasma Phys. **12**, 29 (1986).
[22] V. P. Silin, Sov. Phys. JETP **21**, 1127 (1965); W. L. Kruer, *The Physics of Laser Plasma Interaction*, (Addison-Wesley, New York, 1988).
[23] R. B. Miller, *Intense Charged Particle Beams*, (Plenum Press, N. Y., 1982).